ACS SyntheticBiology

Research Article

pubs.acs.org/synthbio

Model-Driven Engineering of Gene Expression from RNA Replicons

Jacob Beal,*[,†,#] Tyler E. Wagner,[‡,#] Tasuku Kitada,[§] Odisse Azizgolshani,[∥] Jordan Moberg Parker,[⊥] Douglas Densmore,[‡] and Ron Weiss[§]

[†]Raytheon BBN Technologies, Cambridge, Massachusetts United States

[‡]Center of Synthetic Biology, Boston University, Boston, Massachusetts 02215, United States

[§]Department of Biological Engineering, Massachusetts Institute of Technology, Cambridge, Massachusetts 02139, United States

[∥]Department of Chemistry and Biochemistry, University of California Los Angeles, Los Angeles, California 90095-1570, United States

[⊥]Department of Microbiology, Immunology and Molecular Genetics, University of California Los Angeles, 609 Young Drive, Box 148906, Los Angeles, California 90095-1570, United States

Supporting Information

ABSTRACT: RNA replicons are an emerging platform for engineering synthetic biological systems. Replicons self-amplify, can provide persistent high-level expression of proteins even from a small initial dose, and, unlike DNA vectors, pose minimal risk of chromosomal integration. However, no quantitative model sufficient for engineering levels of protein expression from such replicon systems currently exists. Here, we aim to enable the engineering of multigene expression from more than one species of replicon by creating a computational model based on our experimental observations of the expression dynamics in single- and multireplicon systems. To this end, we studied fluorescent protein expression in baby hamster kidney (BHK-21) cells using a replicon derived from Sindbis virus (SINV). We characterized expression dynamics for this platform based on the dose−response of a single species of replicon over 50 h and on a titration of two cotransfected replicons expressing different fluorescent proteins. From this data, we derive a quantitative model of multireplicon expression and validate it by designing a variety of three-replicon systems, with profiles that match desired expression levels. We achieved a mean error of 1.7-fold on a 1000-fold range, thus demonstrating how our model can be applied to precisely control expression levels of each Sindbis replicon species in a system.

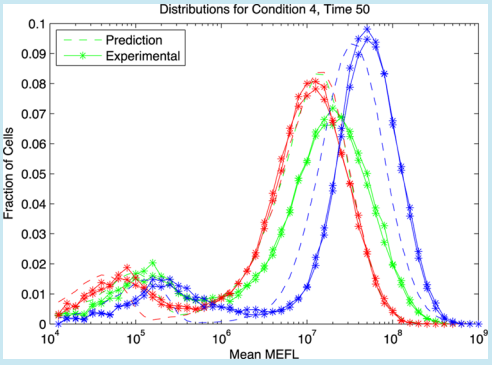

KEYWORDS: *quantitative modeling, circuit prediction, replicon, alphavirus, Sindbis, TASBE characterization, expression control, flow cytometry*

Recently, interest has been growing in RNA replicons as standalone gene delivery vehicles.[1] Two of the primary advantages of replicon-based systems are self-amplification and safety, making replicons an attractive modality for medical applications such as vaccine delivery, gene therapy, and cellular reprogramming.[2−4] Because they are self-amplifying, replicons can generate high expression of a gene product, such as an antigen, from a relatively low initial dose, compared to nonreplicating RNA.[5,6] The self-amplifying feature of replicons is particularly valuable for mammalian systems, in which replicating DNA-based vectors are uncommon and difficult to construct due to their complexity.[7] Moreover, with regard to safety, replicons do not reverse transcribe and are confined to the cytoplasm of the cell, so the risk of undesired integration into the genome is minimal.[8,9]

Of the various replicons that have been developed, we have chosen to focus on a replicon derived from a Sindbis virus (SINV), the most well-characterized alphavirus.[5] Sindbis replicons with reduced cytopathicity and increased duration of expression have been developed.[10−14] SINV is a positive-strand RNA virus with an 11.7 kilobase genome. The SINV genome has a 5′-7-methylguanosine cap and a 3′-poly(A) tail, both of which are characteristics of cellular mRNA, allowing SINV to utilize existing cellular machinery to initiate translation of its nonstructural proteins.[15] The 5′ two-thirds of the SINV genome encodes the four nonstructural proteins that act together to form a replicase complex. Replication occurs through a minus-strand intermediate template, which is used for the synthesis of both the full length positive strand genome, as well as the subgenomic RNA that comprises the 3′ one-third of the genome.[15−18] In the wild type virus, the subgenomic RNA is the source of the structural proteins that allow the virus to propagate to other cells. These structural proteins can be replaced with an engineered sequence to produce alternate gene products, creating a *replicon* (Figure 1a): a general RNA delivery vehicle that amplifies by self-replication, expresses specified gene products, and lacks the

Special Issue: SEED 2014

Received: March 7, 2014
Published: May 30, 2014

DOI: 10.1021/sb500173f
ACS Synth. Biol. 2015, 4, 48−56

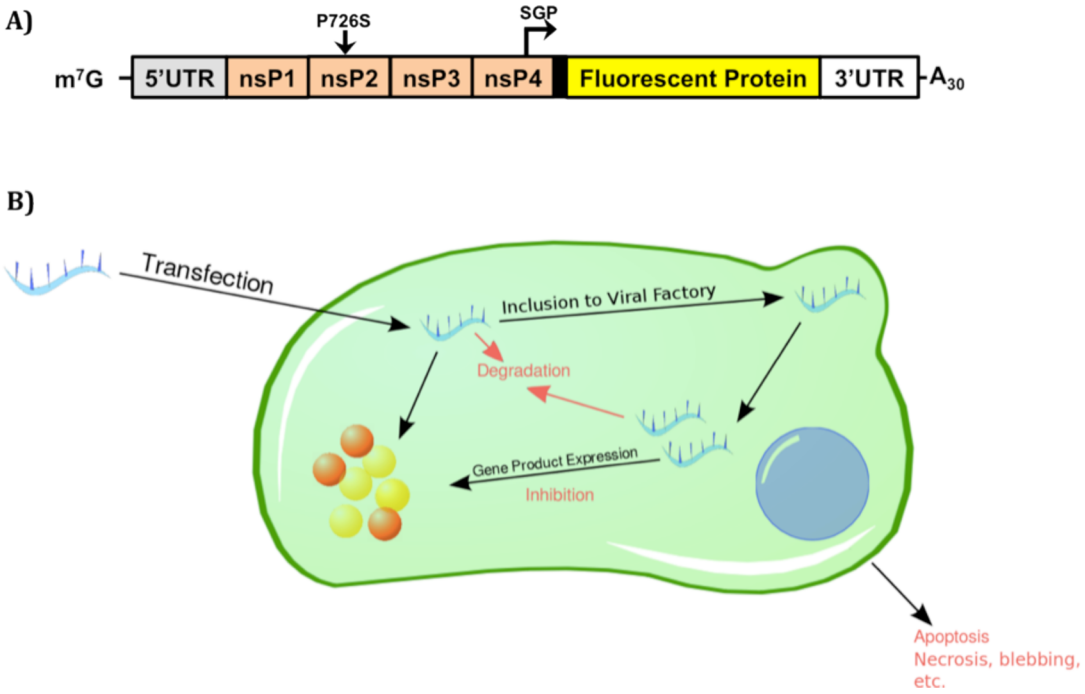

Figure 1. (a) We investigated replicon dynamics using Sindbis replicons with reduced cytopathicity[10] containing the nsP2 P726S mutation (top), in which the portion of the RNA sequence coding for the SINV structural proteins is replaced by an engineered "payload" sequence, such as a fluorescent protein. (b) In replicon-based expression, initially a set of "founder" replicons enter the cell during transfection. The nonstructural proteins (nsPs) expressed from the replicons create "viral factories" in which the number of replicons is amplified exponentially. This process also produces subgenomic transcripts containing the "payload" sequence, which are expressed into proteins. Expression levels may be limited by the ordinary processes of degradation and dilution, as well as resource limits, antiviral innate immune response, and gross cell effects such as apoptosis, necrosis, and blebbing.

necessary structural proteins that would allow it to infect other cells.[19−21]

Initial work using replicon systems has focused mainly on producing a single protein product.[15] Many applications, however, may require more sophisticated replicon-based circuits with multiple gene products at various different expression levels; these products may also need to be separately regulated or to regulate one another. A number of approaches to express multiple genes from replicons have been investigated, including the use of multiple subgenomic promoters,[22−25] insertion of internal ribosome entry sites (IRES),[25−27] and use of 2A sequences.[28−30] Such approaches, however, have a number of limitations, including decreased or uneven expression, RNA recombination, and inherent scaling limits on the size of an effective replicon.[31−33] Moreover, many RNA regulatory mechanisms, such as RNAi or those involving cellular nuclease complexes, operate via RNA degradation and thus will act on the replicon as a whole, thereby preventing the use of these mechanisms in single replicon systems to control individual gene products.[34]

In this manuscript, we adopt an alternate approach based on cotransfection of multiple replicons. With this approach, the coding sequences of a system are distributed onto more than one species of replicon, and the system is installed by mixing these species together in an appropriate titration and cotransfecting. This approach overcomes issues of replicon size and allows each replicon species to be titrated and regulated independently. Similar to multiplasmid systems, however, it introduces variability into the stoichiometry of the system, including the possibility that a cell may receive only part of the system. Precise regulation of a gene product from a single replicon may also benefit from this approach: as we show in this manuscript, single replicon systems tend to saturate to the same final expression level, independent of initial dose, which poses a problem when engineering expression of a single protein product. Using the cotransfection model that we develop in this manuscript, however, the expression of a desired protein can be tuned using a second "ballast replicon" that competes for expression resources.

Thus, we develop cotransfection as a method to enable the precision engineering of protein expression from replicons by constructing a predictive quantitative model of replicon expression dynamics. To this end, we measure the dose−response behavior of a single species of Sindbis replicon in BHK-21 cells over time, and of varying titrations of two cotransfected replicon species. From this data, we derive a quantitative model of multireplicon expression, which we then validate by applying it to design a collection of six three-replicon systems with a range of expression profiles. The experimental behavior of these systems matches our desired expression levels to a mean accuracy of 1.7-fold on a 1000-fold range, thus demonstrating the capability of our model to precisely control gene expression of each Sindbis replicon in a system.

RESULTS

The design of the Sindbis replicons we used and the main processes involved in expression from such replicons are shown in Figure 1. First, the transfection process introduces some number of "founder" replicons into each cell. Using the native translational machinery, these replicons begin to express proteins, specifically a set of nonstructural proteins used for replication. These proteins, through processes not yet fully understood, modify endosomes and lysosomes to create "viral factories" in which they replicate the RNA.[35,36] The replication

DOI: 10.1021/sb500173f
ACS Synth. Biol. 2015, 4, 48−56

process also produces transcripts of the 3′ subgenomic sequence or sequences encoding an engineered "payload," which are translated to express the encoded proteins. These proteins are then degraded by typical cellular mechanisms. Protein expression may be inhibited by type-I interferon (IFN) mediated cellular antiviral innate immune responses,[37] or by gross cellular events such as apoptosis, necrosis, and blebbing. Here, we use BHK-21 cells (an IFN deficient cell line) as the host cell for Sindbis replicon expression to reduce possible complications that the innate immune response may have on gene expression. Expression is also self-regulated by the nonstructural protein complex, which self-cleaves and alters the polarity of the RNA-dependent RNA replication complex.[15]

This mechanistic model implies a set of hypotheses regarding the expression patterns that may be expected in a replicon system with a constitutively expressed stable reporter protein, such as mVenus, mKate, or EBFP2. First, as transfection is a stochastic chemical process, the fraction of cells transfected should be dose-dependent. Moreover, if the replicons are well-mixed and transfections proceed independently (a reasonable null hypothesis), the number of transfections per cell would be expected to follow a Poisson distribution. Possible behaviors range between two asymptotic phases (Figure 2a): a "sparse" phase for lower doses, in which a small fraction of cells are successfully transfected with a single founder replicon and fluoresce, and "dense" phase for higher doses, in which nearly all cells receive many founder replicons and fluoresce. Multireplicon systems will generally need to operate in the "dense" phase such that the probability distributions can be engineered to provide a high likelihood of all replicon species being delivered to each cell with good control of their stoichiometry.

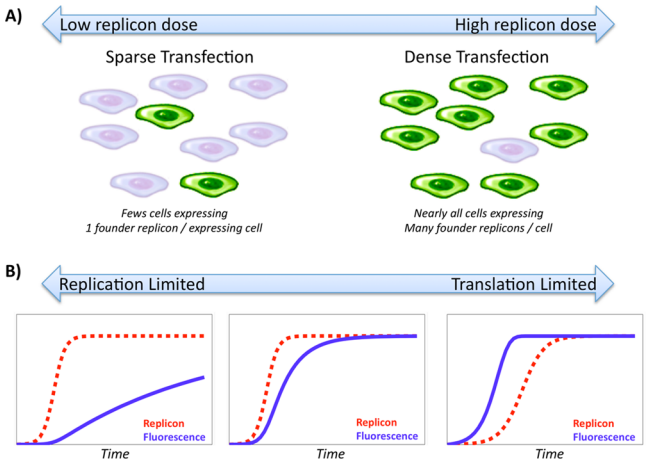

Figure 2. Depending on the relative dose and resources, a replicon system is expected to exhibit qualitatively different phases of behavior. (a) With a very low RNA dose (left), we expect to see only a few cells successfully transfected, and each transfected cell to receive only a single "founder" replicon. At the opposite extreme (right), high doses are expected to put many founder replicons into every cell, in proportion to their fraction of the initial dose. At intermediate levels, most cells will be transfected, but the relative stoichiometry of founder replicons will vary widely. (b) The translation and replication processes are both limited in the amount that they can drive resources. If the replication limit is reached much earlier than the translation limit (left), then expression will rise almost linearly for a long time before slowly reaching an equilibrium. In the opposite extreme, where the translational limit is reached while replication is still proceeding rapidly, then expression will rise exponentially to a sharp limit (right). When both limits are approached at similar rates, expression will rise quickly and then decelerate to an equilibrium. Graphs are ODE simulations varying relative rate constants by approximately 300×, plotted using linear axes.

For those cells that are transfected and fluoresce, the progress of fluorescent protein expression over time will be determined by the relative amount of available resources for replication and translation, or by alternative mechanisms for the reduction of expression, including antiviral innate immune responses or the degradation of RNA (Figure 2b). Replication is expected to initially be exponential, but the number of replicon copies must eventually saturate as either available resources become depleted or the replication process becomes inhibited by itself or the cellular host. At low replicon densities, translation is expected to be linear in the number of copies of the replicon, meaning that during the initial exponential replication phase, fluorescence will rise exponentially, tracking the rise in replicon copies with some delay. If translational resources become depleted or the translation process becomes inhibited, then fluorescence will rapidly converge to a stable expression level. If such a limit is not reached, on the other hand, then fluorescence will continue to increase until protein translation is balanced by dilution and/or decay—a long period of at least several cell divisions or protein half-lives.

Single Replicon Transfection. To determine which of these hypotheses best describes the expression dynamics of Sindbis replicons in BHK-21 cells, we measured the dose–response behavior of cells over the course of 50 h post-transfection (Figure 3a). We transfected BHK-21 cells with Sindbis replicon containing a gene for a fluorescent reporter, mVenus, at logarithmic doses (21, 41, 103, 206, 411, 1027, 2055 ng per 1×10^5 cells). Fluorescence was measured using flow cytometry at 1, 3, 5, 7, 9, 11, 16, 19, 21, 26, 35, and 50 h post-transfection. We found that the transfected population of cells exhibits behavior consistent with being translation-limited, with an extremely sharp rise in mean fluorescence that rapidly saturates. Alternatively, if fluorescent expression were primarily replication-limited, the rate of convergence to saturation would be dominated by the process of achieving equilibrium between production and loss of protein, which should have a time constant on the order of the division time of the cells. Instead, we observe a much faster convergence consistent with translational resource depletion having at least a similar level of importance to replication rates: all dosages converged to a consistent expression level by 16 h and remained relatively stable thereafter (Figure 3a). Before that point, however, there is a monotonic relationship between dose and expression (Figure 3b), suggesting that, at lower dosages, limits on replication are also affecting the course of expression. With this data, we constructed an approximate model of mean protein expression using the following formula derived from the hypothesis that protein expression is strongly regulated by translational resources:

$$E(t) = \max(0, S(1 - 2^{\delta_E - t/\lambda_E}))$$

where $E(t)$ is the expression at time t, S is the saturated expression level, δ_E is an initial delay representing the early phase of the exponential replication process, and λ_E is the time constant on the exponential convergence toward saturation. The delay before significant expression can be observed is due to the delivery and replication process; in principle, we should be able to model the dynamics of the development of viral factories and the dose-dependent rise of expression with respect to time. In this work, however, we restrict our model to the 1-DOF approximation of a fixed delay δ_E (rather than dose-dependent)

DOI: 10.1021/sb500173f
ACS Synth. Biol. 2015, 4, 48–56

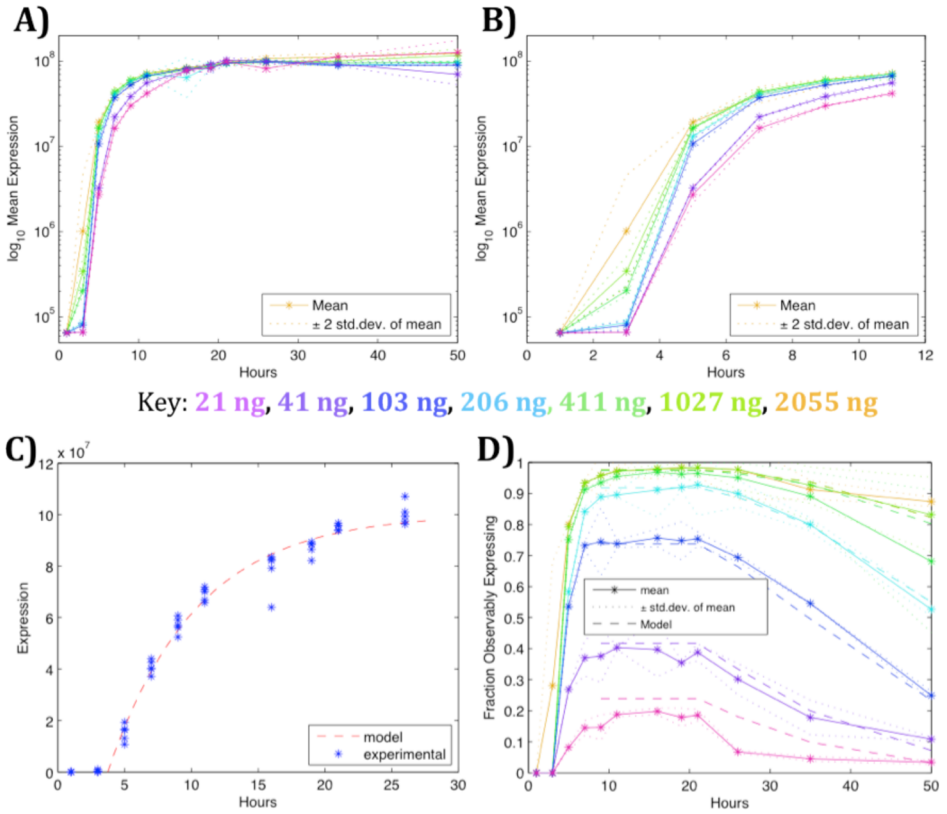

Figure 3. (a) Evolution of fluorescent expression over time for logarithmically varied doses of replicon, showing for all doses a rapid rise toward a consistent dose-independent level. Data shown is mean for upper (transfected) component of bimodal log-normal fit to fluorescence distribution. Dose is indicated by hue, ranging geometrically from 21 ng/μL (magenta) to 2055 ng/μL (yellow). (b) Detail of the first 11 h. (c) The rise toward saturation over the first 26 h shows that observations are well fit by a resource limitation model. (d) The initial fraction of transfected cells is dose-dependent following a Poisson distribution, then decreases as transfected cells stop or drastically slow their rate of division. Expression units are MEFL: molecules of equivalent fluorescein.

because the signal from this process in our data is not sufficient to fit a more complex model within reasonable bounds (Supporting Information section 2), and (as will be seen) abstracting away dose-dependent delay is not the limiting factor on the precision of our predictions.

Figure 3c compares this model (fit to parameters $S = 1.05 \times 10^8$ MEFL, $\delta_E = 4.02$ h, and $\lambda_E = 5.86$ h) against all of the time points gathered through 26 h. The model fits the data well, with the fit having a mean geometric error of 1.07-fold between model and prediction after 5 h, once detectable expression is expected to begin. Note, however, that although this model indicates that expression saturates due to a limit on the translation process, it does not disambiguate between other reasons that translation might decrease or cease, such as resource depletion, innate immune response, or cell death.

The size of the fluorescently expressing population over time can also be predicted from time-course data. Figure 3d shows that the fraction of observably expressing cells versus time is strongly dose dependent. After the first three time points (covering the first 5 h, in which expression is still too low to observe well at most dosages), the fraction of fluorescent cells is stable at first but then begins to decrease. The pattern of decrease is consistent with a model in which replicons are initially distributed into cells following a Poisson distribution (per our mechanistic hypothesis above) and where cells that are not transfected continue to divide, while those that are transfected stop or drastically slow division once replicon and expression levels are high. We thus model the fraction of expressing cells:

$$F(d, 0) = \tau P(\mathrm{Pois}(\alpha d) > 0)$$

$$F(d, t) = \frac{F(d, 0)}{F(d, 0) + (1 - F(d, 0))\cdot \max(1, 2^{\delta_F - t/\lambda_F})}$$

where $F(d,t)$ is the fraction of cells expressing at time t given initial dose d, τ is an ideal transfection efficiency (modeling the fact that some cells may fail to be transfected regardless of dose), $P(\mathrm{Pois}(\alpha d) > 0)$ is the probability of a sample being greater than zero when drawn from a Poisson distribution parametrized by dose times a constant α, δ_F is the delay before cell division is affected in transfected cells, and λ_F is the rate at which untransfected cells out-divide transfected ones. Figure 3d compares this model (fit to parameters $\tau = 0.977$, $\alpha = 0.0127$, $\delta_F = 21.5$ h, and $\lambda_F = 8.89$ h) against time points beginning at 9 h, showing that it is a good fit, with a mean error of 2.5%. Note that although we have quantified the effect on division, it might actually be caused by any number of mechanisms: candidates include resource sequestration, toxicity from the action of the replicon, innate immune response, or some mixture thereof. This data also does not distinguish between failure to divide and slow division: our model only states how much *faster* the untransfected population is dividing than the transfected population.

Another interesting implication of this model is that it appears that no replicon dosage can be low enough to cause this particular replicon/cell system to be primarily limited by replication. Given both the value of α that has been identified

DOI: 10.1021/sb500173f
ACS Synth. Biol. 2015, 4, 48−56

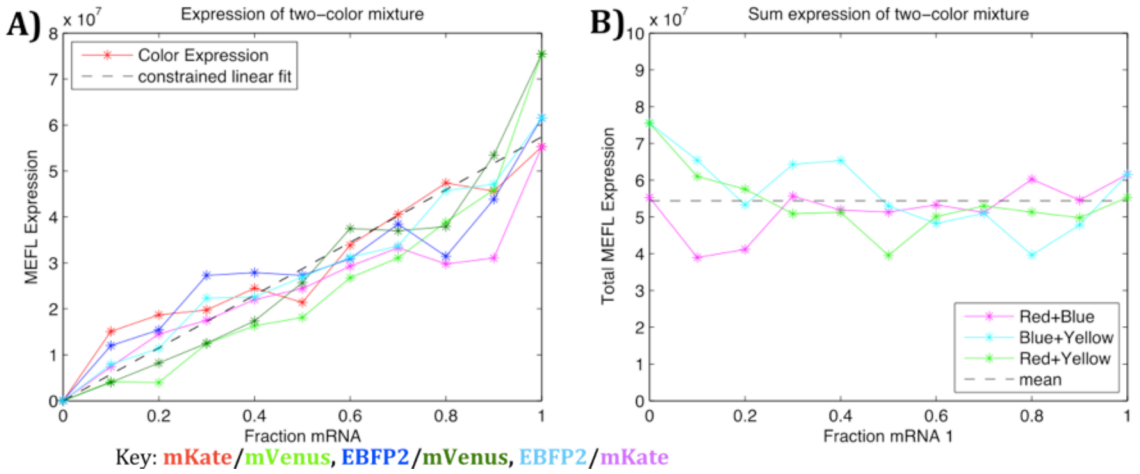

Figure 4. Cotransfection of two replicons at varying titrations and a constant high total dose produces a linear relation between relative dose and fluorescence (a) and a constant total fluorescence (b), as predicted from single-replicon models. Expression units are MEFL: molecules of equivalent fluorescein.

and the large number of nonexpressing cells at low dosage, we may reasonably hypothesize that many cells in the fluorescently expressing population are initially transfected with only a single replicon. In the 21 and 41 ng dose conditions, these cells are expected to make up the vast majority of the expressing population, and in the 103 ng dose condition are expected to be 48% of the expressing population. Thus, further reduction of the initial dose may be expected to further decrease the fraction of expressing cells but will not result in any significant further shift toward expression being primarily limited by replication.

Multi-replicon Transfection. In the discussion above, we established a model that estimates the fraction of cells with active replicons and the mean expression from a single species of replicon within these cells. For engineering systems based on multireplicon cotransfection, however, it will also be important to have a model of the degree of variation anticipated from cell to cell, since small variations in the founder population of replicons may lead to large differences in the relative populations following exponential replication. To quantify variation, we transfected BHK-21 cells with pairs of replicons that are identical except for the choice of fluorescent reporter: mVenus/mKate, mKate/EBFP2, or mVenus/EBFP2. Each sample was transfected with 1390 ng total RNA, at varying titrations of the two replicons ranging from 0% to 100% in steps of 10%. Fluorescence was measured via flow cytometry 20 h post-transfection (Figure 4). Based on our prior models, we expected transfection to be dense, with many founder replicons per cell. By the law of large numbers, this means that the mean fluorescence per cell should be approximately linear with respect to the relative dose (though they may be somewhat distorted by variation) and when converted to equivalent MEFL units the sum of the two fluorescence intensities should be equal to a constant. These predictions are borne out by our observations (Figure 4). We also refine our estimate of S to 5.44×10^7 MEFL using the means of dual transfections, as the geometric means of this collection of high-dose conditions provide a more reliable estimate than the bimodal Gaussian fit used for tracking small expressing populations in the prior experiment.

When considering distribution of fluorescence, however, variation is much greater than can be accounted for only by a pure Poisson distribution. We note two additional sources of variation that are known to have large effects in biological systems. First, most cells (including the BHK-21 cells we are using) vary significantly in their size and state; this is expected to affect both the resources available for expression and the amount of founder population of replicons introduced during transfection. Observing that single-replicon experiments show a log-normal distribution of fluorescence (Supporting Information Figure 1), we model a cell variation factor V as a log-normal distribution:

$$V = 10^{N(0,\sigma)}$$

where $N(0,\sigma)$ is a normal distribution with standard deviation σ. We include this variation factor as a multiplier in the distribution of founder replicons, reflecting the hypothesis that larger cells are likely to take up proportionally more replicons:

$$f_i = \mathrm{Pois}(\alpha V d_i)$$

where f_i is the number of founder replicons of the ith replicon, d_i is the partial dose of the ith replicon, and α is the same parametrization constant that we fit previously in modeling the fraction of transfected cells.

The second major known source of variation is the stochasticity of biochemical processes when there are only a few molecules. In many cases, the number of founder copies of each replicon expected in a given cell may be quite low, in which case the first few replication events may have a large impact on the ultimate ratio of the two cotransfected replicons. This can be modeled mathematically as a Polya Urn process.[38] The Polya Urn process considers an urn that begins with k balls, each of which has some color; for each of n iterations, a ball is drawn, then replaced along with an extra ball of the same color, increasing the number of balls in the urn. This model has the property that when the number of balls is small, the ratios can shift significantly, but as the process continues the ratios drift less, ultimately converging to a value distributed by a β distribution parametrized on the initial set of balls. Applied to model our replicon systems, the colors are the replicon species, the initial balls are the founder copies, and the draw and replacement process is replication events, giving a model of

$$p_i = (1 - \sum_{j<i} p_j)\beta(f_i, \sum_{j>i} f_j)$$

DOI: 10.1021/sb500173f
ACS Synth. Biol. 2015, 4, 48−56

where p_i is the proportion of the ith replicon following replication and $\beta(x,y)$ is the beta distribution.

Note that this model of replication via a Polya Urn process is unlikely to be strongly affected by how replicons are distributed in viral factories, the process by which viral factories are formed, or the process by which RNA escapes the viral factories. Independent factories, each replicating its own collection of replicons, may be viewed as members of a "meta-urn" that produces the same distribution of converged ratios, as long as it is the case that many replicons can fit in a factory. Likewise, independent factories may be translated in time without a significant effect, as long as the variance in the time to form a factory is not so long as to allow other factories to significantly affect the available transcriptional resources. From our results, it appears that neither of these cases holds strongly enough to prevent the Polya Urn model from being a reasonable approximation of observed behavior. This does not, however, constrain the system enough to shed any significant new light on the behavior of viral factories.

Combining these factors, we enhance our earlier model of mean protein expression for single replicons to a model giving a distribution of expression for multiple replicon species:

$$E(t, i) = Vp_i \max(0, S(1 - 2^{\delta_E - t/\lambda_E}))$$

with the expression $E(t,i)$ of the ith replicon at time t varying from the mean according to the cell variation factor and the distribution of the replicons' proportions implied by the initial dose. Fitting this model against the set of 90%/10% titrations (to maximize observed variation), we obtain $\sigma = 0.365$ (Figure 5).

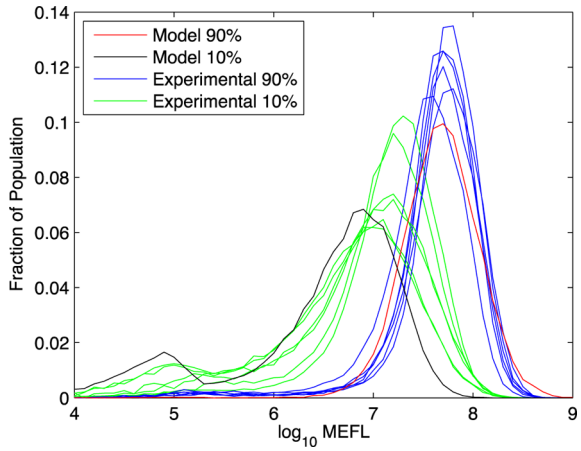

Figure 5. Experimental observations vs model of fluorescence distribution for all 10%:90% ratios of two-replicon transfection, in all six dosage/color combinations.

Engineering Multi-replicon Systems. We validated our expression model, as well as demonstrated how it can be used to engineer precision control of expression levels, by designing and predicting expression for a set of six three-replicon mixtures. These six mixture conditions, shown in Table 1, were chosen to evaluate the performance of our expression model on a variety of systems with dosage levels and dosage ratios ranging across approximately 2 orders of magnitude. BHK-21 cells were transfected with each replicon mixture at the specified dosages and fluorescence was measured by flow cytometry at 3, 6, 11, 20, 26, 34, and 50 h post-transfection. In all cases, our expression model provides a highly precise prediction of the observed value, with a mean prediction error of only 1.7-fold (Figure 6a). With respect to individual mixtures, there is no significant difference in prediction quality (Figure 6b). With respect to time, prediction errors are slightly lower at around 24 h, when the greatest number of cells are fluorescing most strongly, but show no significant pattern for when predictions are better or worse (Supporting Information Figure 2). Means versus time for each mixture are shown in Figure 6c and Supporting Information Figure 3. Finally, the expression model predicts well not only the mean but also the distributions of fluorescence within each sample (Figure 6d and Supporting Information Figures 4–10).

Table 1. Dosages for Three-Replicon Mixtures Used for Validation of Model-Driven Design

condition	mVenus (ng)	mKate (ng)	EBFP2 (ng)
1	180	180	180
2	540	540	540
3	180	900	720
4	360	360	1080
5	18	180	900
6	720	36	36

DISCUSSION

The work presented in this manuscript enables the use of RNA replicons as a predictable platform for synthetic biology. We have demonstrated that Sindbis replicon in BHK-21 cells has a highly systematic pattern of gene product expression over time. Expression can be predicted with high precision from the initial replicon dosage, using an 8-DOF model. This model was derived from the basic mechanisms of transfection, replication, and translation, and parametrized using experimental observation of single- and dual-replicon transfections. Our model allows predictive engineering of a multireplicon system, as we have demonstrated by designing and precisely predicting the expression distributions of a collection of six mixtures of three replicons across a wide range of dosages and ratios.

The same approach can be applied to precision control of the expression from a single-replicon system, by titrating with a competing "ballast" replicon (note that changing the initial dosage of a single replicon does not change the per-cell expression level after the first few hours, only the fraction of cells successfully transfected). Although our work enables the immediate engineering of a wide range of RNA replicon expression systems, further investigation is necessary to support a full range of replicon-based applications. At present, our models only apply to constitutive expression from replicons of uniform size, with similar sized products, under control of identical subgenomic promoters. Replicons of different sizes may replicate at different rates, which would change the mapping from founder population to the distribution of converged ratios. Similarly, different gene products may require different resources, which may affect their share of the translational limit, and differences in subgenomic promoters are also expected to affect expression. Regulatory interactions between replicons will also affect expression dynamics, particularly when the mechanism of regulation involves RNA degradation. Finally, the nonstructural proteins of the replicon are translated as well; these are not included in our model at present because their effect can be factored out for constitutive expression from uniform replicons. However, if these nonstructural proteins have a significant effect on expression, they too may need to be included in a more general computational model. In many cases, extending models to cover such systems is also likely to require a more explicit

DOI: 10.1021/sb500173f
ACS Synth. Biol. 2015, 4, 48–56

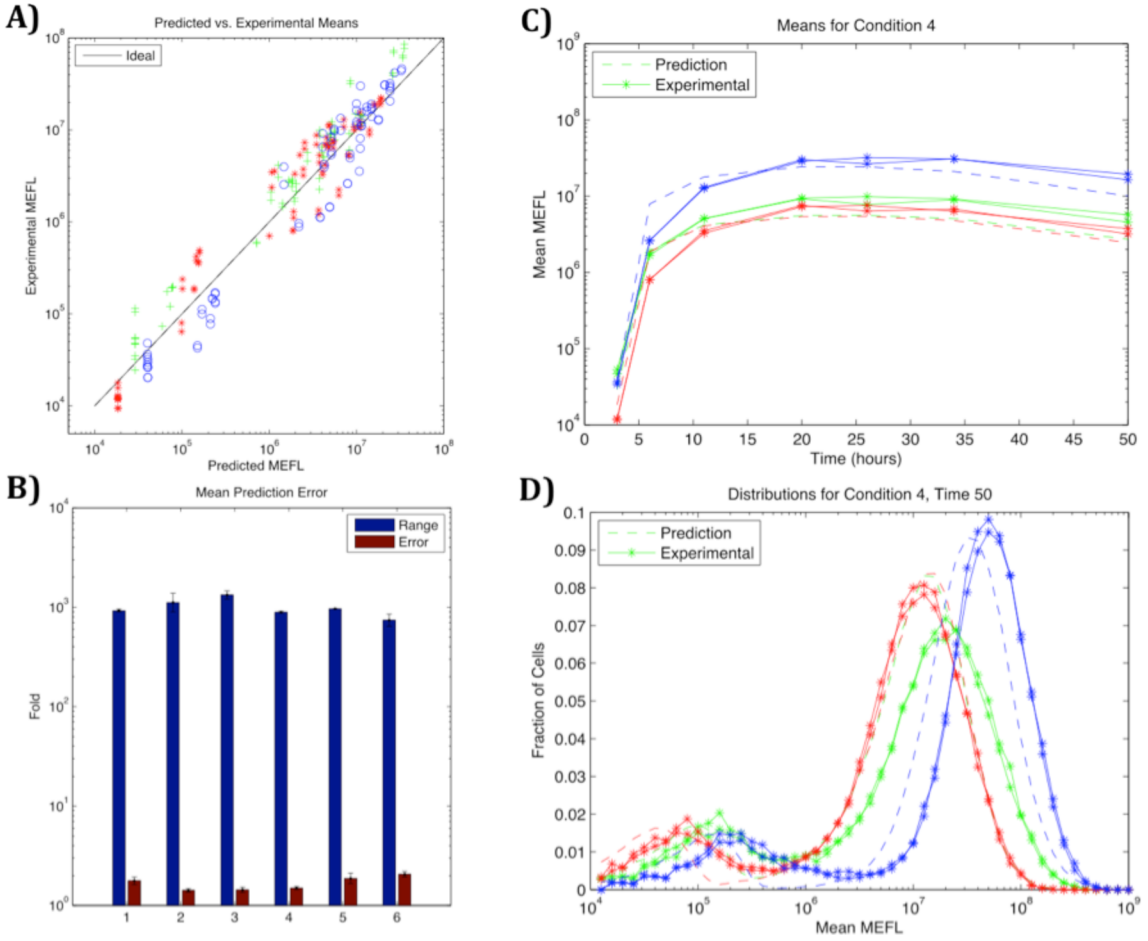

Figure 6. Our Sindbis/BHK expression model successfully predicts the evolution of expression distributions for six three-replicon mixtures across a wide range of initial dosages: (a) mean predicted vs measured expression for each color for all time/mixture combinations measured (mKate is red, EBFP2 is blue, and mVenus is green); (b) geometric mean fold error vs fold expression range for each of the six mixtures. Standard deviation is across replicates for range and across replicates and colors for error. (c, d) Examples of prediction detail: (c) predicted vs experimental evolution of mean expression for Mixture 4 (360 ng mVenus, 360 ng mKate, 1080 ng EBFP2) for 50 h post-transfection; (d) predicted vs experimental distribution of fluorescence values for Mixture 4 at 50 h post-transfection. Full details of predictions are shown in Supporting Information Figure 2 through 10. Expression units are MEFL: molecules of equivalent fluorescein.

model of replication than the current coarse abstraction. Although the parameters of the system that we studied precluded building a comprehensive quantitative model from fluorescence data, such a model should be able to be acquired either from other replicons with lower levels of protein expression or by studying RNA levels directly, for example, via qRT-PCR. Understanding the contributions of different mechanisms to the translation limit will also be important for future engineering work.

A concern for certain applications is the fact that the BHK-21 cells stopped or drastically slowed dividing *in vitro*, which indicates gross cell effects that may preclude the use of Sindbis replicons in many therapeutic applications. However, other combinations of replicons and cell lines may show less impact, and published reports of sustained *in vivo* replicon expression are quite promising.[39] Since other replicon/cell combinations are generally expected to have the same underlying biochemical processes (except for the immune mechanisms that BHK-21 lacks), we expect that the same general models will likely apply, though they will have different parameter values.

In summary, the methods and approach that we have presented here provide a solid foundation for developing a general capability for precision engineering of biological systems using RNA replicons. Beyond replicons, this work also provides an example of systematic establishment of a quantitative engineering method for a biological mechanism, some principles of which may be able to be extended more broadly to other biological systems, such as DNA-based transcriptional and translational gene circuits. Our model construction depends critically on the use of per-cell measurements, which allow distinction between expressing and nonexpressing subpopulations and expose systematic effects that would otherwise not be directly observable. It also depends on being able to translate all fluorescence measurements into equivalent absolute units, which allows data from different fluorescent proteins to be compared directly in the two-replicon titration experiments. Finally, we abstract mechanisms where necessary in order to ensure that all parameters used by our model are well-supported by experimental data. Applying such methods in other contexts may likewise assist in the more general development of improved biological engineering models and methods.

METHODS

Cloning/RNA Generation. All Sindbis constructs were created from pSINV-EYFP using standard molecular cloning techniques.[40] The replicon itself originated from the TE12 strain

DOI: 10.1021/sb500173f
ACS Synth. Biol. 2015, 4, 48−56

of Sindbis and was altered to contain the previously characterized, less cytopathic P726S mutation in nsP2.[10,11] The plasmids were linearized using SacI prior to *in vitro* transcription using the mMESSAGE mMachine SP6 Kit (Life Technologies). The resulting RNA was purified using the RNeasy Mini Kit (Qiagen) and the concentration was measured using the NanoDrop 2000.

Transfection. All Sindbis transfections were conducted in BHK-21 cells (a kind gift from Dr. James H. Strauss) cultured in EMEM (ATCC) supplemented with 10% FBS (PAA) at 37 °C and 5% CO_2. BHK-21 cells at approximately 70% confluence were electroporated using the Neon Transfection System (Life Technologies) following optimization, according to the manufacturers' instructions. In general, for a single well of a 24-well plate (Corning), approximately 100 000 cells were electroporated with RNA ranging from 18 to 2055 ng.

For the time-course experiment, samples were taken in duplicate. For the dual transfection experiment, one sample was taken for each titration, with the single replicon samples (100%/0% titration) shared between color pairings. For the three-replicon mixtures, samples were taken in duplicate. Note that the statistical strength of results is not significantly weakened by using smaller numbers of samples per condition, due to the fact that conclusions are drawn from the joint analysis of groups of samples across varying conditions.

Flow Cytometry. Cells for each time point were washed with 1× PBS, trypsinized, and resuspended in 1× PBS. Flow cytometry was performed using the BD LSRFortessa Flow Cytometer System and FACSDiva software was used for initial data collection.

Statistical Analysis and Modeling. Flow cytometry data was converted from arbitrary units to compensated MEFL (Molecules of Equivalent FLuorescein) using the TASBE characterization method.[41] An affine compensation matrix is computed from single positive and blank controls. FITC measurements are calibrated to MEFL using SpheroTech RCP-30-5-A beads,[42] and mappings from other channels to equivalent FITC are computed from cotransfection of high equal dose (>500 ng) of replicons identical except for the choice of fluorescent protein. For dual transfection data, we use the 50:50 condition for each pair; for mixture data we use the 26-h time point for condition 2. For Figure 3, expression data is fit against a bimodal Gaussian on the log scale to distinguish the subpopulation of cells where the replicon is successfully transfected from the subpopulation where it is not. Unlike gating thresholds, a bimodal Gaussian model allows good estimation of relative population sizes even when subpopulations overlap in their distribution of expression. Mean of expressing population is then calculated as the mean of the upper component of a bimodal log-normal fit to the observed distribution, except for time points 35 and 50 of lowest dosage, where expressing population is too small for a good fit, and we instead select the distribution peak at highest MEFL. For all other figures, where mixture of replicons skews distributions away from log-normal, means are computed as geometric mean of all samples $>10^4$ MEFL. Histograms are generated by segmenting MEFL data into logarithmic bins at 10 bins/decade, with geometric mean and variance computed for those data points in each bin. Model fits are performed using standard least-squares curve fitting on a linear scale. The model of expression rising to saturation is fit against all but the two lowest dosages, which appear to be significantly affected by replication dynamics. The model of fraction transfected is fit against all but the lowest dosage, where expression was too low in some cases for bimodal Gaussian fits to converge. All parameter estimates are expressed to three significant figures for consistency.

■ ASSOCIATED CONTENT

Supporting Information

List of exceptions to replicate numbers, a discussion of choices in modeling replication, replicon sequences, and full details of all predictions. This material is available free of charge *via* the Internet at http://pubs.acs.org.

■ AUTHOR INFORMATION

Corresponding Author

*Email: jakebeal@bbn.com.

Author Contributions

#J.B. and T.E.W. contributed equally to this work. J.B., T.E.W., and R.W. designed experiments. T.E.W. performed the experiments; T.K. assisted with experiments and performed preliminary experiments. J.B. developed and applied computational analysis methods, developed computational models, and developed methods for prediction and design of expression. J.B., T.E.W., R.W., and T.K. interpreted results. O.A. and J.M.P. supplied the replicon and expertise with the Sindbis replicon system. T.K. supplied source DNA constructs. J.B. and T.E.W. wrote the manuscript; all authors edited the manuscript.

Notes

The authors declare no competing financial interest.

■ ACKNOWLEDGMENTS

The authors thank John Scarpa for preparing Figure 1b (using TinkerCell software, found at http://www.tinkercell.com/Home/cite) and Andrey Krivoy for input into discussions. The work presented in this manuscript was supported by DARPA under grant W911NF-11-054.

■ ABBREVIATIONS

MEFL,molecules of equivalent fluorescein; EBFP2,enhanced blue fluorescent protein

■ REFERENCES

(1) Lundstrom, K. (2009) Alphaviruses in Gene Therapy. *Viruses 1*, 13−25.

(2) Lundstrom, K. (2012) Alphavirus Vectors in Vaccine Development. *J. Vaccines Vaccin.* 3 DOI: 10.4172/2157-7560.1000139.

(3) Wahlfors, J. J., Zullo, S. A., Loimas, S., Nelson, D. M., and Morgan, R. A. (2000) Evaluation of recombinant alphaviruses as vectors in gene therapy. *Gene Ther. 7*, 472 DOI: 101038sjgt3301122.

(4) Yoshioka, N., Gros, E., Li, H.-R., Kumar, S., Deacon, D. C., Maron, C., Muotri, A. R., Chi, N. C., Fu, X.-D., Yu, B. D., and Dowdy, S. F. (2013) Efficient generation of human iPSCs by a synthetic self-replicative RNA. *Cell Stem Cell 13*, 246−254.

(5) Xiong, C., Levis, R., Shen, P., Schlesinger, S., Rice, C. M., and Huang, H. V. (1989) Sindbis virus: An efficient, broad host range vector for gene expression in animal cells. *Science 243*, 1188−1191.

(6) Kulasegaran-Shylini, R., Thiviyanathan, V., Gorenstein, D. G., and Frolov, I. (2009) The 5′UTR-specific mutation in VEEV TC-83 genome has a strong effect on RNA replication and subgenomic RNA synthesis, but not on translation of the encoded proteins. *Virology 387*, 211−221.

(7) Kouprina, N., Earnshaw, W. C., Masumoto, H., and Larionov, V. (2013) A new generation of human artificial chromosomes for functional genomics and gene therapy. *Cell. Mol. Life Sci. CMLS 70*, 1135−1148.

(8) Robertson, J. S. (1994) Safety considerations for nucleic acid vaccines. *Vaccine 12*, 1526−1528.

DOI: 10.1021/sb500173f
ACS Synth. Biol. 2015, 4, 48−56

(9) Klinman, D. M., Takeno, M., Ichino, M., Gu, M., Yamshchikov, G., Mor, G., and Conover, J. (1997) DNA vaccines: Safety and efficacy issues. *Springer Semin. Immunopathol. 19*, 245−256.
(10) Frolov, I., Agapov, E., Hoffman, T. A., Prágai, B. M., Lippa, M., Schlesinger, S., and Rice, C. M. (1999) Selection of RNA replicons capable of persistent noncytopathic replication in mammalian cells. *J. Virol. 73*, 3854−3865.
(11) Lustig, S., Jackson, A. C., Hahn, C. S., Griffin, D. E., Strauss, E. G., and Strauss, J. H. (1988) Molecular basis of Sindbis virus neurovirulence in mice. *J. Virol. 62*, 2329−2336.
(12) Heise, M. T., White, L. J., Simpson, D. A., Leonard, C., Bernard, K. A., Meeker, R. B., and Johnston, R. E. (2003) An attenuating mutation in nsP1 of the Sindbis-group virus S.A.AR86 accelerates nonstructural protein processing and up-regulates viral 26S RNA synthesis. *J. Virol. 77*, 1149−1156.
(13) Dryga, S. A., Dryga, O. A., and Schlesinger, S. (1997) Identification of mutations in a Sindbis virus variant able to establish persistent infection in BHK Cells: The importance of a mutation in the nsP2 gene. *Virology 228*, 74−83.
(14) Perri, S., Driver, D. A., Gardner, J. P., Sherrill, S., Belli, B. A., Dubensky, T. W., and Polo, J. M. (2000) Replicon vectors derived from Sindbis virus and Semliki Forest virus that establish persistent replication in host cells. *J. Virol. 74*, 9802−9807.
(15) Strauss, J. H., and Strauss, E. G. (1994) The alphaviruses: Gene expression, replication, and evolution. *Microbiol. Rev. 58*, 491−562.
(16) Hardy, W. R., and Strauss, J. H. (1989) Processing the nonstructural polyproteins of sindbis virus: Nonstructural proteinase is in the C-terminal half of nsP2 and functions both in cis and in trans. *J. Virol. 63*, 4653−4664.
(17) Shirako, Y., and Strauss, J. H. (1990) Cleavage between nsP1 and nsP2 initiates the processing pathway of Sindbis virus nonstructural polyprotein P123. *Virology 177*, 54−64.
(18) Jose, J., Snyder, J. E., and Kuhn, R. J. (2009) A structural and functional perspective of alphavirus replication and assembly. *Future Microbiol. 4*, 837−856.
(19) Schlesinger, S., and Dubensky, T. W., Jr. (1999) Alphavirus vectors for gene expression and vaccines. *Curr. Opin. Biotechnol. 10*, 434−439.
(20) Agapov, E. V., Frolov, I., Lindenbach, B. D., Pragai, B. M., Schlesinger, S., and Rice, C. M. (1998) Noncytopathic Sindbis virus RNA vectors for heterologous gene expression. *Proc. Natl. Acad. Sci. U.S.A. 95*, 12989−12994.
(21) Geall, A. J., Verma, A., Otten, G. R., Shaw, C. A., Hekele, A., Banerjee, K., Cu, Y., Beard, C. W., Brito, L. A., Krucker, T., O'Hagan, D. T., Singh, M., Mason, P. W., Valiante, N. M., Dormitzer, P. R., Barnett, S. W., Rappuoli, R., Ulmer, J. B., and Mandl, C. W. (2012) Nonviral delivery of self-amplifying RNA vaccines. *Proc. Natl. Acad. Sci. U.S.A. 109*, 14604−14609.
(22) Hahn, C. S., Hahn, Y. S., Braciale, T. J., and Rice, C. M. (1992) Infectious Sindbis virus transient expression vectors for studying antigen processing and presentation. *Proc. Natl. Acad. Sci. U.S.A. 89*, 2679−2683.
(23) Frolov, I., Hoffman, T. A., Pragai, B. M., Dryga, S. A., Huang, H. V., Schlesinger, S., and Rice, C. M. (1996) Alphavirus-based expression vectors: Strategies and applications. *Proc. Natl. Acad. Sci. U.S.A. 93*, 11371−11377.
(24) Petrakova, O., Volkova, E., Gorchakov, R., Paessler, S., Kinney, R. M., and Frolov, I. (2005) Noncytopathic replication of venezuelan equine encephalitis virus and eastern equine encephalitis virus replicons in mammalian cells. *J. Virol. 79*, 7597−7608.
(25) Wiley, M. R., Roberts, L. O., Adelman, Z. N., Myles, K. M. (2010) Double subgenomic alphaviruses expressing multiple fluorescent proteins using a *Rhopalosiphum padi* virus internal ribosome entry site element. *PLoS One 5*.
(26) Sanz, M. Á., Castelló, A., Ventoso, I., Berlanga, J. J., and Carrasco, L. (2009) Dual Mechanism for the Translation of Subgenomic mRNA from Sindbis Virus in Infected and Uninfected Cells. *PLoS One 4*, e4772.
(27) Firth, A. E., and Brierley, I. (2012) Non-canonical translation in RNA viruses. *J. Gen. Virol. 93*, 1385−1409.
(28) Donnelly, M. L. L., Luke, G., Mehrotra, A., Li, X., Hughes, L. E., Gani, D., and Ryan, M. D. (2001) Analysis of the aphthovirus 2A/2B polyprotein "cleavage" mechanism indicates not a proteolytic reaction, but a novel translational effect: A putative ribosomal "skip. *J. Gen. Virol. 82*, 1013−1025.
(29) Thomas, J. M., Klimstra, W. B., Ryman, K. D., and Heidner, H. W. (2003) Sindbis virus vectors designed to express a foreign protein as a cleavable component of the viral structural polyprotein. *J. Virol. 77*, 5598−5606.
(30) Kim, J. H., Lee, S.-R., Li, L.-H., Park, H.-J., Park, J.-H., Lee, K. Y., Kim, M.-K., Shin, B. A., Choi, S.-Y. (2011) High cleavage efficiency of a 2A peptide derived from porcine teschovirus-1 in human cell lines, zebrafish, and mice. *PLoS One 6*.
(31) Frolov, I., and Schlesinger, S. (1994) Translation of Sindbis virus mRNA: Effects of sequences downstream of the initiating codon. *J. Virol. 68*, 8111−8117.
(32) Caley, I. J., Betts, M. R., Davis, N. L., Swanstrom, R., Frelinger, J. A., and Johnston, R. E. (1999) Venezuelan equine encephalitis virus vectors expressing HIV-1 proteins: Vector design strategies for improved vaccine efficacy. *Vaccine 17*, 3124−3135.
(33) Kallio, K., Hellström, K., Balistreri, G., Spuul, P., Jokitalo, E., and Ahola, T. (2013) Template RNA length determines the size of replication complex spherules for Semliki Forest virus. *J. Virol. 87*, 9125−9134.
(34) Decker, C. J., and Parker, R. (2012) P-bodies and stress granules: Possible roles in the control of translation and mRNA degradation. *Cold Spring Harb. Perspect. Biol. 4*, a012286.
(35) Wengler, G., Koschinski, A., Wengler, G., and Dreyer, F. (2003) Entry of alphaviruses at the plasma membrane converts the viral surface proteins into an ion-permeable pore that can be detected by electrophysiological analyses of whole-cell membrane currents. *J. Gen. Virol. 84*, 173−181.
(36) Paul, D., and Bartenschlager, R. (2013) Architecture and biogenesis of plus-strand RNA virus replication factories. *World J. Virol. 2*, 32−48.
(37) Perri, S., Greer, C. E., Thudium, K., Doe, B., Legg, H., Liu, H., Romero, R. E., Tang, Z., Bin, Q., Dubensky, T. W., Vajdy, M., Otten, G. R., and Polo, J. M. (2003) An alphavirus replicon particle chimera derived from venezuelan equine encephalitis and sindbis viruses is a potent gene-based vaccine delivery vector. *J. Virol. 77*, 10394−10403.
(38) Mahmoud, H. (2008) *Polya Urn Models*. CRC Press, Boca Raton, FL.
(39) Petrakova, O., Volkova, E., Gorchakov, R., Paessler, S., Kinney, R. M., and Frolov, I. (2005) Noncytopathic replication of Venezuelan equine encephalitis virus and eastern equine encephalitis virus replicons in Mammalian cells. *J. Virol. 79*, 7597−7608.
(40) Azizgolshani, O., Garmann, R. F., Cadena-Nava, R., Knobler, C. M., and Gelbart, W. M. (2013) Reconstituted plant viral capsids can release genes to mammalian cells. *Virology 441*, 12−17.
(41) Beal, J.; Weiss, R.; Yaman, F.; Davidsohn, N.; Adler, A. *A Method for Fast, High-Precision Characterization of Synthetic Biology Devices*; Computer Science and Artificial Intelligence Laboratory Technical Report; MIT: Cambridge, MA, 2012
(42) Perfetto, S. P., Ambrozak, D., Nguyen, R., Chattopadhyay, P., and Roederer, M. (2006) Quality assurance for polychromatic flow cytometry. *Nat. Protoc. 1*, 1522−1530.

DOI: 10.1021/sb500173f
ACS Synth. Biol. 2015, 4, 48−56